Published in final edited form as:
Nature. 2008 May 8; 453(7192): 184–189. doi:10.1038/nature06941.

Dynamic binding orientations direct activity of HIV reverse transcriptase

Elio A. Abbondanzieri[1,*], **Gregory Bokinsky**[1,*], **Jason W. Rausch**[4], **Jennifer X. Zhang**[1], **Stuart F. J. Le Grice**[4], and **Xiaowei Zhuang**[1,2,3]

1 *Department of Chemistry and Chemical Biology, Harvard University, Cambridge, MA 02138, USA*

2 *Department of Physics, Harvard University, Cambridge, MA 02138, USA*

3 *Howard Hughes Medical Institute, Harvard University, Cambridge, MA 02138, USA*

4 *HIV Drug Resistance Program, National Cancer Institute, Frederick, MD 21702, USA*

Abstract

The reverse transcriptase of human immunodeficiency virus (HIV) catalyzes a series of reactions to convert the single-stranded RNA genome of HIV into double-stranded DNA for host-cell integration. This task requires the multifunctional reverse transcriptase to discriminate a variety of nucleic-acid substrates such that active sites of the enzyme are correctly positioned to support one of three catalytic functions: RNA-directed DNA synthesis, DNA-directed DNA synthesis and DNA-directed RNA hydrolysis. However, the mechanism by which substrates regulate reverse transcriptase activities remains unclear. Here, we report distinct orientational dynamics of reverse transcriptase observed on different substrates using a single-molecule assay. The enzyme adopted opposite binding orientations on duplexes containing DNA or RNA primers, directing its DNA synthesis or RNA hydrolysis activity, respectively. On duplexes containing the HIV polypurine tracts, unique RNA primers for the plus-strand DNA synthesis, the enzyme can bind in both orientations and rapidly switch between the two states. The switching kinetics were regulated by cognate nucleotides and non-nucleoside reverse transcriptase inhibitors, a major class of anti-HIV drugs. These results indicate that the enzymatic activities of reverse transcriptase are determined by its binding orientation on substrates.

Virtually all RNA- and DNA-processing enzymes exhibit selectivity for backbone compositions or base sequences of their nucleic-acid substrates. This substrate selectivity is especially critical for the HIV-1 reverse transcriptase (RT), which binds and discriminates a variety of nucleic-acid duplexes for distinct catalytic functions[1,2]. RT is a heterodimer consisting of a p51 and a p66 subunit, the latter of which contains catalytically active DNA polymerase and RNase H domains[3,4], catalyzing a complex, multi-step reaction to convert the single-stranded RNA genome into double-stranded DNA[1,2]. First, RT uses the viral RNA genome as a template and a host-cell tRNA as a primer to synthesize a minus-strand DNA, producing an RNA/DNA hybrid[5–7]. This duplex becomes the substrate of the RNase H domain of RT, which cleaves the RNA strand at numerous points, leaving behind short RNA stretches hybridized to the nascent DNA[8–10]. Among these RNAs, two specific purine-rich sequences, known as the polypurine tracts (PPTs), serve as unique primers to initiate the plus-strand DNA synthesis[11–13], thereby creating the double-stranded DNA viral genome. Specific RNase H cleavage then removes the PPT primers and exposes the integration sequence to facilitate

Correspondence and requests for materials should be addressed to X.Z. (zhuang@chemistry.harvard.edu).
*These authors contributed equally to this work.

insertion of the viral DNA into the host chromosome[14]. Inappropriate initiation of the plus-strand DNA synthesis at other RNA stretches prevents integration[2,15]. RT must therefore obey a primer-selection rule: (1) DNA primers readily engage the polymerase activity of RT; (2) generic RNA primers are not efficiently extended by RT but readily engage the RNase H activity of RT when annealed with DNA; (3) the PPT RNA can direct both the DNA polymerase activity and a site-specific RNase H activity of RT. The mechanism by which RT discriminates among these substrates and executes the appropriate catalytic function is, however, poorly understood. While RNase H cleavage analysis suggest the presence of different interaction modes of RT with substrates[16,17], crystal structures to date have revealed only one enzyme binding orientation[4,18–22].

Single-molecule assay for enzyme-substrate interactions

To better understand how RT interactions with substrates, we designed a single-molecule assay to measure the enzyme orientation relative to its substrate using Förster resonance energy transfer (FRET)[23,24], a method well suited for probing dynamic protein-nucleic acid interactions[25–27]. Static FRET measurements have also been used previously to characterize the pre-and post-translocation states of RT on a DNA duplex[28]. Because RT accommodates 19–22 base pairs of nucleic-acid duplex within its primer-template binding cleft[19,22,29] (Fig. 1a), we constructed several duplex substrates with different backbone compositions and base sequences, each consisting of a 50 nucleotide (nt) oligonucleotide mimicking the template and a complementary 19–21 nt oligonucleotide emulating the primer (Fig. 1b and Supplementary Fig. 1). A Cy5 fluorophore was specifically attached to one of the single-stranded overhang regions on the template to serve as the FRET acceptor. We refer to the labelling schemes with Cy5 near the 5′ and 3′ ends of the primer as the 5* or 3* labels, respectively.

Surface-immobilized substrates were immersed in a solution containing RT molecules labelled with a FRET donor dye Cy3 either at the RNase H domain (H-labelled) or at the fingers domain (F-labelled) of the p66 subunit (Fig. 1a). The two dye-labelling sites were located on opposite poles of the enzyme and separated by ~8 nm. An E478Q mutation was introduced to the RNase H domain to abolish its RNA cleavage activity so as to prevent the RT-induced degradation of nucleic-acid substrates during observation[30]. Experiments were conducted with this RNase H-inactive variant unless otherwise mentioned. Neither dye attachment nor surface immobilization significantly altered the polymerase activity of RT (Supplementary Fig. 2).

Fluorescence of individual duplex substrates on the slide was monitored using total-internal-reflection fluorescence (TIRF) microscopy with alternating laser excitations[25] at 532 nm and 635 nm (Fig. 1c). The 532 nm light excites the FRET donor Cy3 without significantly exciting the acceptor Cy5, allowing us to detect the FRET between the Cy3-labelled RT and the Cy5-labeled substrate. The 635 nm light directly excites the Cy5 dye, providing a means to probe the presence of the nucleic-acid substrate and FRET acceptor independent of RT binding. Freely diffusing RT was observed to bind and dissociate from the substrates in real time. Each binding event caused an increase in the total fluorescence signal collected from both Cy3 and Cy5 channels under the 532 nm excitation without affecting the signal obtained under the 635 nm excitation (Fig. 1d). The observed FRET value allowed the enzyme orientation of each binding event to be determined.

RT binds to DNA and RNA primers in opposite orientations

We first examined the binding orientation of RT on a 19 nt DNA primer hybridized to a 50 nt DNA template. When H-labelled RT was added to the 5*-labelled substrates, binding events consistently yielded high FRET values (centred at ~0.94) (Fig. 2a), indicating an overwhelming tendency for the enzyme to bind with its RNase H domain close to the 5′ terminus of the primer. Conversely, predominantly low FRET values (~ 0.14) were observed when H-labelled RT

bound to an isogenic 3*-labelled substrate (Fig 2b). Furthermore, F-labelled RT primarily bound to the 3*-labelled substrate with high FRET values (~ 0.90, Fig. 2c), indicating that the DNA polymerase domain was located near the 3′ end of the primer. As a control, when both Cy3 and Cy5 were placed on the substrates, either near the same end of or flanking the duplex region, no significant change in FRET was observed upon RT addition, suggesting that RT does not cause a sizable change in the photo-physical properties of the dyes or the end-to-end distance of the duplex (Supplementary Fig. 3). Taken together, these results indicate that RT binds to the DNA-DNA primer-template complex with its polymerase active site between the fingers and palm domains close to the 3′ end of the primer and RNase H domain near the 5′ end - an orientation that matches the polymerization-competent binding mode observed in RT-substrate co-crystal structures[19–22]. A virtually identical binding orientation was observed for RT on a 19 nt DNA primer annealed to a 50 nt RNA template (Supplementary Fig. 4). The same binding orientation was also observed for the RNase H active RT (without the E478Q mutation) on the DNA-DNA primer-template complex (Supplementary Fig. 5)

Next, we examined binding to an RNA primer annealed to a DNA template. The primer and template sequences were identical to those used above. Again, RT predominately adopted a single binding configuration, but now with a drastically different orientation: H-labelled RT bound to the 5*-labelled substrates with low FRET values (~ 0.27, Fig. 2d) but to the 3*-labelled substrates with primarily high FRET values (~ 0.95, Fig.2e); F-labelled RT bound to 5*-labelled substrate with high FRET values (~ 0.88, Fig.2f). These results unambiguously define a binding orientation on the RNA primer that is opposite to that on the DNA primer, with the DNA polymerase domain adjacent to the 5′ terminus of the primer and the RNase H domain close to the 3′ end. The same binding orientation was also found for the RNase H active RT (Supplementary Fig. 5). This orientation clearly cannot support primer extension activity, but directly explains the primary RNase H-cleavage mode observed previously on similar substrates, in which the cleavage site is 18 nucleotide from the 5′ terminus of the RNA[17]. The two opposite binding orientations on DNA and RNA primers were also observed on primers encoding an alternate sequence (supplementary Fig. 6).

To identify which features were most important in discriminating between DNA and RNA primers and directing RT orientation, we designed a series of 19 nt chimeric primers containing different compositions of RNA and DNA nucleotides denoted by xR:yD (i.e. x RNA nt at the 5′-end and y DNA nt at the 3′-end). These chimeras were annealed to a 50 nt DNA template and incubated with H-labelled RT (Fig. 3a and supplementary Fig. 7). Whereas pure DNA and RNA primers bound to RT predominantly in a single orientation, most chimeric primers supported both high and low FRET orientations (supplementary Fig. 7). The free energy difference (ΔG) between the two states was most sensitive to the sugar composition of the 4 – 5 nucleotides located at each end of the 19 nt primer (Fig. 3b), suggesting that the interactions between RT and nucleic acid at opposite ends of the primer-template binding cleft were most important in determining the binding orientation. This observation is consistent with the crystal structures, which show RT-substrate contacts primarily clustered in two regions near the DNA polymerase and RNase H active sites[19,22]. Remarkably, a single nucleotide provided the strongest determinant of binding orientation: changing the sugar content of the 5th nucleotide from the primer 5′ terminus alone caused a nearly 2 k_BT change in ΔG (Fig. 3b). This position makes specific contacts with RT residues T473 and Q475 located within the RNase H primer grip[19,22]. These residues are conserved among RNases H found in viruses, bacteria and human[22,31,32]. Alanine substitution of these two residues in HIV-1 RT reduces the DNA synthesis rate and inhibits virus infectivity[33]. Overall, the backbone composition of nucleotides at the 5′ end of the primer played a greater role in determining enzyme binding orientation than those at the 3′ end (Fig. 3b). To further test this notion, we constructed a new chimeric primer 9D:10R (i.e. 5′-proximal DNA, 3′-proximal RNA), which has the same DNA to RNA ratio as the 10R:9D primer but with different 5′ end backbone composition. As

expected, the 9D:10R and 10R:9D primers supported opposite binding orientations of RT that closely resembled the orientational distributions of RT bound to pure DNA and RNA primers, respectively (Fig. 3a).

Enzyme binding orientation determines the enzymatic activity of RT

The observation that RT bound to the DNA and RNA primers with opposite orientations suggests an interesting hypothesis: that primer extension activity is determined by the binding orientation of the enzyme. To test this model, we probed the DNA polymerase activity of RT on the DNA (19D) and RNA (19R) primers as well as the chimeric primers 9D:10R and 10R:9D, each annealed to a 50 nt DNA template (supplementary Fig. 8 and Fig. 4a). Remarkably, RT was capable of extending the 3′ end of both 19D and 9D:10R rapidly, with a rate comparable to previously reported steady-state extension rates of DNA primers[34,35], even though the 9D:10R primer contained a ribonucleotide sugar backbone at its 3′ terminus. Polymerase activity was strongly inhibited for both 19R and 10R:9D. Furthermore, the rate of primer extension correlated with the fraction of time that the RT enzyme bound in the polymerase-component orientation (Fig. 4b). These results indicate that the binding orientation is the strongest determinant of the primer-extension activity, whereas the content of the sugar-phosphate backbone contacting the DNA polymerase active site is less important for synthesis activity. Our results also suggest a surprising allosteric effect where contacts between the 5′ end of the primer and the RNase H primer grip regulate the DNA polymerase activity by determining the orientation of the enzyme on the substrate.

Dynamic binding orientations of RT on PPT substrates

While RNA primers do not generally support initiation of DNA synthesis by RT, two copies of 15 nt RNA purine sequences, referred to as the PPTs, uniquely serve as primers for plus-strand DNA synthesis[2,11–13,15]. During infection, RT cleaves precisely at the 3′ terminus of the PPT, allowing DNA synthesis to be initiated at this position. The enzyme then removes the PPT primer by cleaving at its junction with and the nascent DNA[2,15]. How RT interacts with the PPT to support both DNA polymerase and RNase H activities remains a mystery. To address this question, we constructed three oligonucleotides encoding the PPT sequence to mimic different stages in plus-strand DNA synthesis. To simulate a PPT sequence that has not yet been cleaved at its 3′ terminus, we introduced a 2 nt RNA extension, creating the PPT:r2 RNA. Similarly, the PPT:d2 chimera (containing a 2 nt DNA extension) was used to emulate a plus-strand primer from which DNA synthesis has already started. These primers were annealed to a 50 nt DNA template and assayed for RT binding (Figs. 5a–c). The FRET distribution of RT bound to the PPT:r2 primer-template complex was quantitatively similar to that observed in the case of a non-specific RNA primer (compare Fig. 5a with Fig. 2d), suggesting that RT was predominantly bound in a cleavage orientation. In contrast, on the PPT and PPT:d2 substrates, RT spent a substantial portion of time in the high FRET, polymerization-competent orientation (Figs. 5b, c). These data suggest that the priming activity of the PPT for plus-strand DNA synthesis originates from its unique ability among RNA sequences to direct RT binding in a polymerase-competent orientation.

On the substrates that support both DNA polymerase and RNase H competent orientations, including the PPT, PPT:d2 and chimeric RNA:DNA primers, RT exhibited spontaneous transitions between these two orientations and flipping transitions were observed with different labelling schemes (Fig. 5d and supplementary Fig. 9). The flipping transition did not appear to require the binding of multiple enzymes, as the flipping kinetics were independent of the RT concentration. The observation of flipping transitions within a single binding event is surprising considering the extensive network of contacts between the RT and its substrates[19,22].

Cognate nucleotide and non-nucleoside RT inhibitor regulate the binding orientation of RT

To explore the flipping mechanism, we investigated the effect of small molecules, including dNTP and non-nucleoside RT inhibitors (NNRTIs), on the equilibrium and rate constants of the flipping transitions using the PPT:d2 primer or a modified primer containing a chain terminating di-deoxyribonucleotide (PPT:dd2). Addition of dTTP, the next cognate nucleotide for primer extension, stabilized the high FRET, polymerase-competent orientation of RT (Figs. 5d, e). The stabilization magnitude increased with dTTP concentration over a physiologically relevant range (Fig. 5e). Kinetically, addition of 1 mM of dTTP decreased the rate constant of flipping from the high FRET to the low FRET orientation, $k_{high\text{-}low}$, by 20 fold without substantially affecting the reverse rate $k_{low\text{-}high}$ (Supplementary Fig. 10). In contrast, addition of a mismatched nucleotide (dCTP) did not induce a similar effect (Supplementary Fig. 11).

NNRTIs are clinically approved anti-HIV drugs[36] that bind to a hydrophobic pocket[4] near the polymerase active site of RT to inhibit DNA synthesis allosterically[37]. We examined one such NNRTI, Nevirapine, for its effects on the orientational dynamics of RT. Nevirapine appeared to have an opposite effect as compared to cognate dNTP. Addition of Nevirapine significantly destabilized the high-FRET, polymerase-competent orientation (Figs. 5d, f): the presence of the drug caused a 3.5 fold increase in the flipping rate from the high to the low FRET orientation, $k_{high\text{-}low}$, but without significantly altering the reverse rate $k_{low\text{-}high}$ (Supplementary Fig. 10). A similar effect was observed for a separate NNRTI, Efavirenz. These results provide a structural basis for the previously observed specific inhibition of the PPT-initiated plus-strand DNA synthesis by NNRTIs, which occurs at a 40 fold lower concentration of NNRTI than that required for the inhibition of minus-strand DNA synthesis[38].

Discussion

We have developed a single-molecule FRET assay to monitor the interactions between HIV RT and its nucleic-acid substrates in real time. These experiments directly revealed two opposite orientations with which the RT enzyme binds to DNA and RNA primers. The primary determinant of the enzyme orientation is the sugar backbone composition of the 4 – 5 nucleotides at each end of the primer, located within the polymerase and RNase H primer grip regions of the RT binding cleft. The primer-extension activity of RT is quantitatively correlated with the enzyme orientation, providing a structural basis for the primer-selection rule of RT.

Remarkably, the enzyme can bind to the special PPT RNA sequence, which directs the transition from minus-strand to plus-strand synthesis, in both orientations. Furthermore, the enzyme can flip spontaneously between the two states despite the extensive contact between RT and its nucleic-acid substrates. The flipping kinetics were altered by both cognate nucleotides and non-nucleoside RT inhibitors, but the two types of small molecules had opposite effects. While the addition of cognate nucleotides caused a drastic decrease in the flipping rate from the polymerase-competent to the RNase H-competent orientation, the NNRTI substantially increased the same rate constant. NNRTIs and dNTPs have been shown to have opposite effects on the structural dynamics of the fingers and thumb subdomains[20]: while dNTPs bring these regions closer together to form a tighter clamp on the nucleic-acid substrate, NNRTIs cause further separation of the two sub-domains. Our data thus suggest a potential pathway for the flipping transition that requires relaxation of the “grip” formed by the fingers and thumb sub-domains around the nucleic-acid substrate. This spontaneous structural reorganization of the RT-substrate complex potentially allows the enzyme to rapidly explore multiple binding orientations that support distinct functions, thereby increasing replication efficacy.

METHODS SUMMARY

For single-molecule measurements of RT interactions with nucleic acids, the dye-labelled nucleic-acid substrates were immobilized on the PEG-coated fused quartz slides via a biotin-streptavidin linkage. Binding of the dye-labelled RT molecules in solution to the immobilized substrates was monitored using the TIRF imaging geometry with alternating 532 nm and 635 nm excitations[25]. FRET histograms were constructed from binding events of hundreds of molecules. To calculate the free energy difference between high and low FRET states, these histograms were fit to a double Gaussian function and the ΔG value was determined from the ratio between the areas under the two Gaussian peaks. Within each binding event, high FRET and low FRET sub-states were identified, and the lifetimes of the binding events and the sub-states were recorded. These lifetimes were combined with a simple kinetic model to derive the rate constants of transition between the sub-states as well as the rate of dissociation from each sub-state.

Supplementary Material

Refer to Web version on PubMed Central for supplementary material.

Acknowledgements

The authors thank Jenny Miller for providing initial samples of RT and Shixin Liu for helpful discussions. This work is supported in part by NIH (GM 068518) and Packard Foundation (to X.Z.) and the Intramural Research Program of the Centre for Cancer Research, NCI (to S.F.J.L.G.) X.Z. is a Howard Hughes Medical Institute investigator. E.A.A. is a Jane Coffin Childs postdoctoral fellow. Nevirapine and Efavirenz were provided through the AIDS Research and Reference Reagent Program of the National Institutes of Health.

References

1. Goff, Stephen P. Fields Virology. Knipe, DM.; Howley, PM., editors. Vol. 2. Lippincott Williams and Wilkins; Philadelphia: 2001. p. 1871-1940.
2. Champoux, JJ. Reverse Transcriptase. Skalka, AM.; Goff, SP., editors. Cold Spring Harbor Laboratory Press; New York: 1993. p. 10-118.
3. Hostomsky Z, Hostomska Z, Fu TB, Taylor J. Reverse transcriptase of human immunodeficiency virus type 1: functionality of subunits of the heterodimer in DNA synthesis. J Virol 1992;66:3179–3182. [PubMed: 1373206]
4. Kohlstaedt LA, Wang J, Friedman JM, Rice PA, Steitz TA. Crystal structure at 3.5 A resolution of HIV-1 reverse transcriptase complexed with an inhibitor. Science 1992;256:1783–1790. [PubMed: 1377403]
5. Baltimore D. Viral RNA-dependent DNA Polymerase: RNA-dependent DNA Polymerase in Virions of RNA Tumour Viruses. Nature 1970;226:1209–1211. [PubMed: 4316300]
6. Temin AM, Mizutani S. Viral RNA-dependent DNA Polymerase: RNA-dependent DNA Polymerase in Virions of Rous Sarcoma Virus. Nature 1970;226:1211–1213. [PubMed: 4316301]
7. Aiyar A, Cobrinik D, Ge Z, Kung HJ, Leis J. Interaction between retroviral-u5 RNA and the t-psi-c loop of the transfer RNAtrp primer is required for efficient initiation of reverse transcription. J Virol 1992;66:2464–2472. [PubMed: 1548772]
8. Leis JP, Berkower I, Hurwitz J. RNA-dependent DNA polymerase-activity of RNA tumor-viruses. 5 Mechanism of action of ribonuclease H isolated from avian myeloblastosis virus and Escherichia-coli. Proc Natl Acad Sci USA 1973;70:466–470. [PubMed: 4119789]
9. Hansen J, Schulze T, Mellert W, Moelling K. Identification and characterization of HIV-specific RNase H by monoclonal antibody. EMBO J 1988;7:239–243. [PubMed: 2452083]
10. Tanese N, Telesnitsky A, Goff SP. Abortive reverse transcription by mutants of moloney murine leukemia-virus deficient in the reverse transcriptase-associated RNase H-function. J Virol 1991;65:4387–4397. [PubMed: 1712862]

11. Finston WI, Champoux JJ. RNA-primed initiation of moloney murine leukemia-virus plus strands by reverse-transcriptase in vitro. J Virol 1984;51:26–33. [PubMed: 6202882]
12. Omer CA, Resnick R, Faras AJ. Evidence for involvement of an RNA primer in initiation of strong-stop plus DNA-synthesis during reverse transcription in vitro. J Virol 1984;50:465–470. [PubMed: 6200608]
13. Huber HE, Richardson CC. Processing of the primer for plus strand DNA-synthesis by human immunodeficiency virus-1 reverse-transcriptase. J Biol Chem 1990;265:10565–10573. [PubMed: 1693920]
14. Schultz SJ, Zhang MH, Kelleher CD, Champoux JJ. Analysis of plus-strand primer selection, removal, and reutilization by retroviral reverse transcriptases. J Biol Chem 2000;275:32299–32309. [PubMed: 10913435]
15. Rausch JW, Le Grice SF. 'Binding, bending and bonding': polypurine tract-primed initiation of plus-strand DNA synthesis in human immunodeficiency virus. Int J Biochem Cell Biol 2004;36:1752–1766. [PubMed: 15183342]
16. Gopalakrishnan V, Peliska JA, Benkovic SJ. Human-immunodeficiency-virus type-1 reverse-transcriptase - spatial and temporal relationship between the polymerase and RNase-H activities. Proc Natl Acad Sci USA 1992;89:10763–10767. [PubMed: 1279694]
17. Wisniewski M, Balakrishnan M, Palaniappan C, Fay PJ, Bambara RA. Unique progressive cleavage mechanism of HIV reverse transcriptase RNase H. Proc Natl Acad Sci USA 2000;97:11978–11983. [PubMed: 11035788]
18. Arnold E, et al. Structure of hiv-1 reverse-transcriptase DNA complex at 7-a resolution showing active-site locations. Nature 1992;357:85–89. [PubMed: 1374166]
19. Ding J, et al. Structure and functional implications of the polymerase active site region in a complex of HIV-1 RT with a double-stranded DNA template-primer and an antibody Fab fragment at 2.8 A resolution. J Mol Biol 1998;284:1095–1111. [PubMed: 9837729]
20. Huang H, Chopra R, Verdine GL, Harrison SC. Structure of a covalently trapped catalytic complex of HIV-1 reverse transcriptase: implications for drug resistance. Science 1998;282:1669–1675. [PubMed: 9831551]
21. Sarafianos SG, et al. Structures of HIV-1 reverse transcriptase with pre- and post-translocation AZTMP-terminated DNA. EMBO J 2002;21:6614–6624. [PubMed: 12456667]
22. Sarafianos SG, et al. Crystal structure of HIV-1 reverse transcriptase in complex with a polypurine tract RNA:DNA. EMBO J 2001;20:1449–1461. [PubMed: 11250910]
23. Stryer L, Haugland RP. Energy transfer: a spectroscopic ruler. Proc Natl Acad Sci USA 1967;58:719–726. [PubMed: 5233469]
24. Ha T, et al. Probing the interaction between two single molecules: fluorescence resonance energy transfer between a single donor and a single acceptor. Proc Natl Acad Sci USA 1996;93:6264–6268. [PubMed: 8692803]
25. Kapanidis AN, et al. Initial transcription by RNA polymerase proceeds through a DNA-scrunching mechanism. Science 2006;314:1144–1147. [PubMed: 17110578]
26. Stone MD, et al. Stepwise protein-mediated RNA folding directs assembly of telomerase ribonucleoprotein. Nature 2007;446:458–461. [PubMed: 17322903]
27. Myong S, Bruno MM, Pyle AM, Ha T. Spring-loaded mechanism of DNA unwinding by hepatitis C virus NS3 helicase. Science 2007;317:513–516. [PubMed: 17656723]
28. Rothwell PJ, et al. Multiparameter single-molecule fluorescence spectroscopy reveals heterogeneity of HIV-1 reverse transcriptase:primer/template complexes. Proc Natl Acad Sci USA 2003;100:1655–1660. [PubMed: 12578980]
29. Metzger W, Hermann T, Schatz O, Le Grice SF, Heumann H. Hydroxyl radical footprint analysis of human immunodeficiency virus reverse transcriptase-template primer complexes. Proc Natl Acad Sci USA 1993;90:5909–5913. [PubMed: 7687057]
30. Schatz O, Cromme FV, Gruninger-Leitch F, Le Grice SF. Point mutations in conserved amino acid residues within the C-terminal domain of HIV-1 reverse transcriptase specifically repress RNase H function. FEBS letters 1989;257:311–314. [PubMed: 2479577]

31. Nowotny M, Gaidamakov SA, Crouch RJ, Yang W. Crystal structures of RNase H bound to an RNA/DNA hybrid: substrate specificity and metal-dependent catalysis. Cell 2005;121:1005–1016. [PubMed: 15989951]

32. Nowotny M, et al. Structure of human RNase H1 complexed with an RNA/DNA hybrid: insight into HIV reverse transcription. Mol Cell 2007;28:264–276. [PubMed: 17964265]

33. Julias JG, McWilliams MJ, Sarafianos SG, Arnold E, Hughes SH. Mutations in the RNase H domain of HIV-1 reverse transcriptase affect the initiation of DNA synthesis and the specificity of RNase H cleavage in vivo. Proc Natl Acad Sci USA 2002;99:9515–9520. [PubMed: 12093908]

34. Hsieh JC, Zinnen S, Modrich P. Kinetic mechanism of the DNA-dependent DNA polymerase activity of human immunodeficiency virus reverse transcriptase. J Biol Chem 1993;268:24607–24613. [PubMed: 7693703]

35. Kati WM, Johnson KA, Jerva LF, Anderson KS. Mechanism and fidelity of HIV reverse transcriptase. J Biol Chem 1992;267:25988–25997. [PubMed: 1281479]

36. El Safadi Y, Vivet-Boudou V, Marquet R. HIV-1 reverse transcriptase inhibitors. Appl Microbiol Biotechnol 2007;75:723–737. [PubMed: 17370068]

37. Spence RA, Kati WM, Anderson KS, Johnson KA. Mechanism of inhibition of HIV-1 reverse transcriptase by nonnucleoside inhibitors. Science 1995;267:988–993. [PubMed: 7532321]

38. Grobler JA, et al. HIV-1 reverse transcriptase plus-strand initiation exhibits preferential sensitivity to non-nucleoside reverse transcriptase inhibitors in vitro. J Biol Chem 2007;282:8005–8010. [PubMed: 17172472]

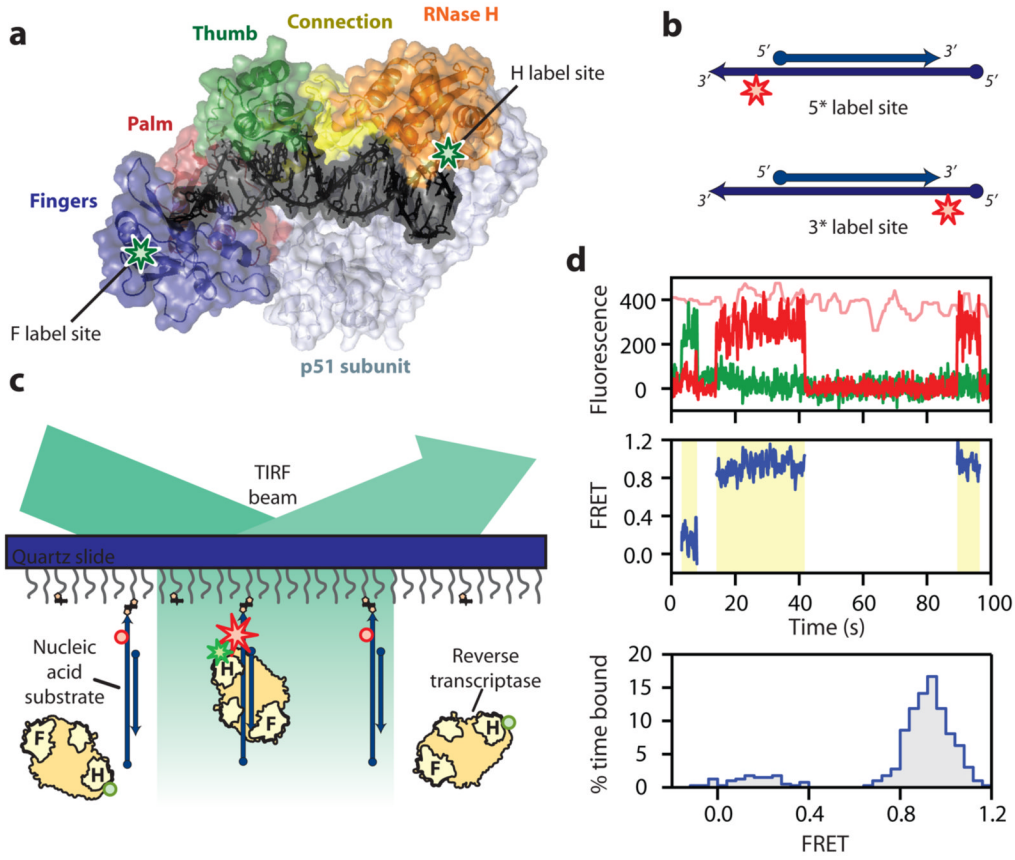

Figure 1. Single-molecule FRET assay for probing the orientational dynamics of RT

a, The structure of HIV-1 RT bound to a DNA-DNA substrate[21]. Labelling sites for Cy3 on RT are highlighted by green stars. **b**, Nucleic-acid substrates consisted of a 19–21 nt primer strand annealed to a 50 nt template strand containing an Cy5 label (red star). Cy5 was either 3 nt from the 5′ end (circle) or 4–6 nt from the 3′ end (arrow) of the primer. **c**, Single-molecule detection of Cy3 (green star or sphere) labelled RT binding to and dissociating from the surface-immobilized nucleic-acid substrates labelled with Cy5 (red star or sphere). The stars and spheres indicated dyes that do or do not emit fluorescence, respectively. **d**, FRET analysis for RT binding to a single primer-template complex: The upper panel shows the fluorescence time traces from Cy3 (green) and Cy5 (red) under 532 nm excitation and that from Cy5 (pink) under 635 nm excitation. The FRET value is calculated over the duration of the binding events (middle panel, yellow shaded regions) and a FRET distribution histogram is created for the binding events (lower panel).

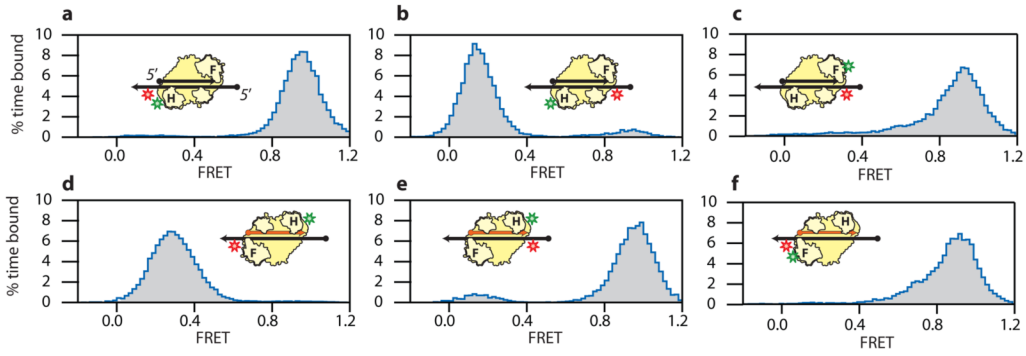

Figure 2. FRET distributions of RT bound to nucleic-acid substrates reveal distinct RT binding orientations on RNA and DNA primers

a, RT with Cy3 (green star) attached in the H-labelling scheme was allowed to bind substrates consisting of DNA primer and template (black arrow), with Cy5 (red star) attached in the 5*-labelling scheme. **b**, H-labelled RT bound to 3*-labelled DNA duplex substrates. **c**, F-labelled RT bound to 3*-labelled DNA duplex substrates. **d**, H-labelled RT bound to 5*-labelled hybrid duplex substrates consisting of a RNA primer (orange arrow) and a DNA template (black arrow). **e**, H-labelled RT bound to 3*-labelled hybrid duplex substrates. **f**, F-labelled RT bound to 5*-labelled hybrid duplex substrates. The RT binding orientations consistent with the FRET distributions are depicted.

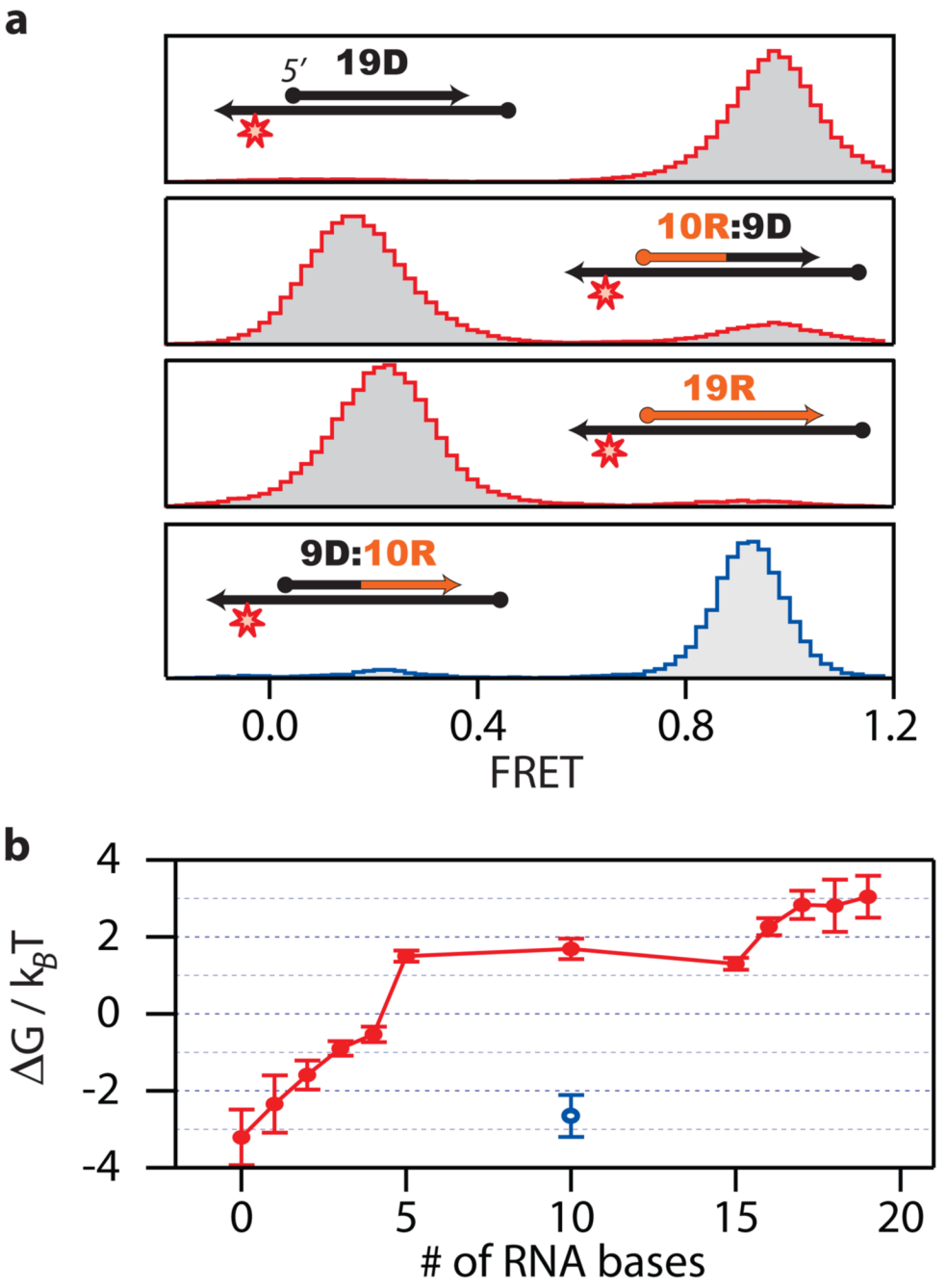

Figure 3. Binding orientation of RT on chimeric substrates

a, Selected FRET distributions of H-labelled RT bound to 5*-labelled substrates containing various 19 nt chimeric RNA:DNA primers hybridized to a DNA template. FRET distributions of other xR:yD substrates are shown in supplementary Fig. 7. **b**, The free energy difference ΔG between the high and low FRET orientations is plotted as a function of RNA content for both xR:yD (red) and 9D:10R (blue) chimeras. The error bars are the standard error of the mean (N = 3).

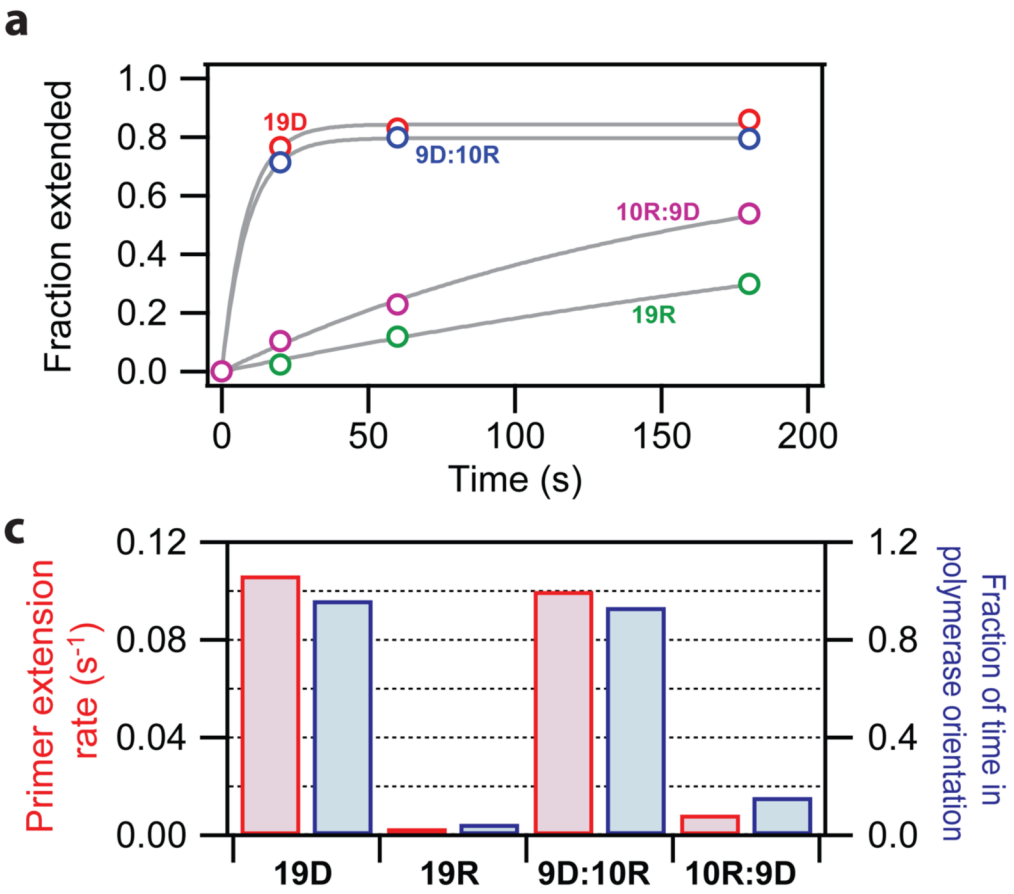

Figure 4. The DNA polymerase activity of RT correlates with its binding orientation on substrates

a, Primer extension activity of RT assayed on four selected primers (19D, 19R, 9D:10R and 10R:9D) annealed to a DNA template. The fraction of primers which had been extended by more than one bases is plotted as a function of time for the four primers (coloured circles). The data were fit to a single-exponential decay (grey lines) to deduce the primer extension rate constants. **b**, Rate constants of primer extension (red) correlate with the fractional of time the RT bound in the high FRET orientation conducive to polymerization (blue).

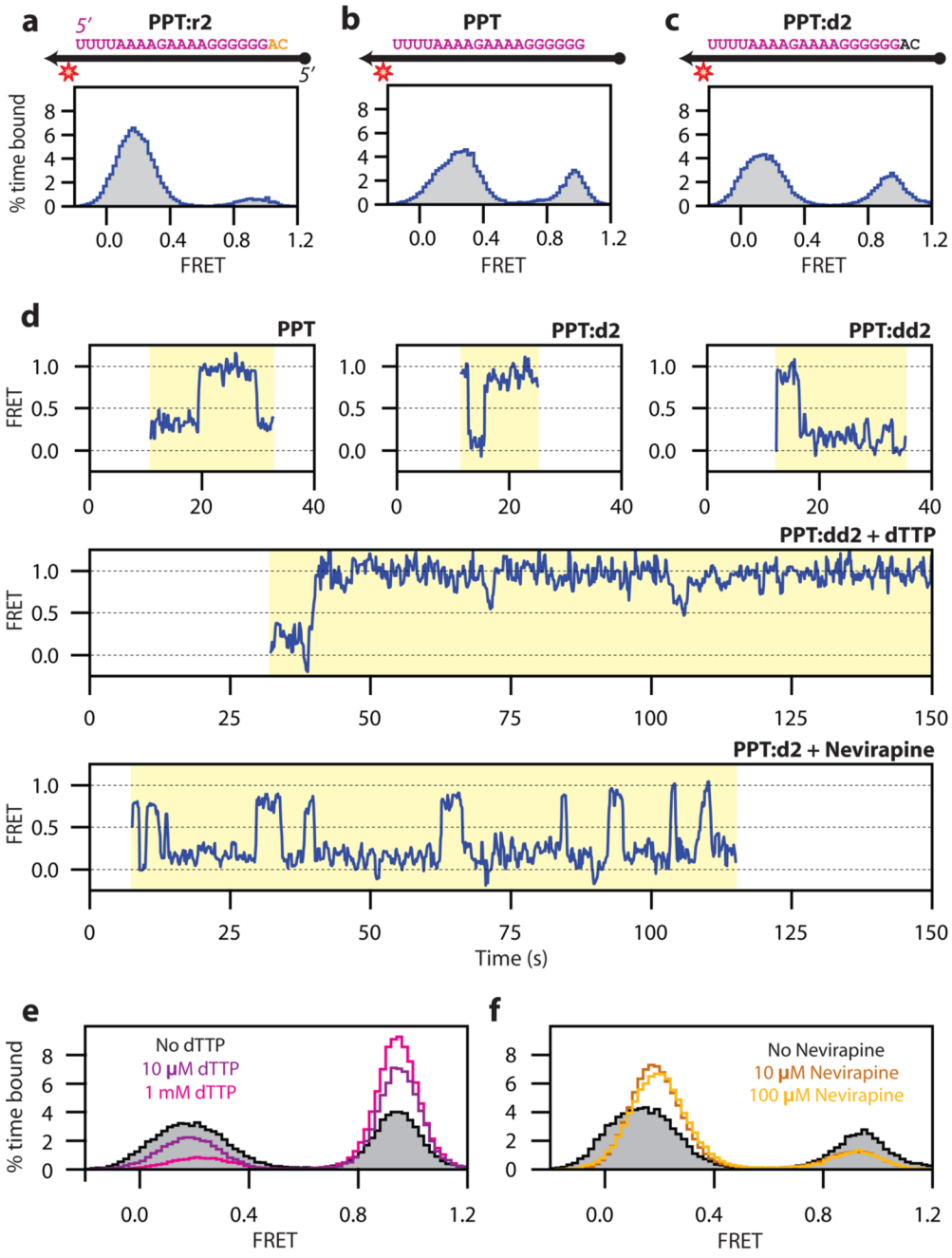

Figure 5. Dynamic binding orientations of RT on PPT substrates

a-c, FRET histograms of H-labelled RT bound to substrates containing 5*-labelled PPT:r2, PPT or PPT:d2 primers annealed to DNA templates. The PPT sequence is highlighted in violet letters and the 2 nt RNA and DNA extensions are coloured in orange and black, respectively. The DNA template is shown as a black arrow. **d**, FRET time traces of RT bound to PPT, PPT:d2, and PPT:dd2 substrates showed spontaneous flipping transitions between the two binding orientations. **e**, FRET histograms of RT bound to PPT:dd2 substrates in the presence of 0, 10 μM, and 1 mM dTTP. **f**, FRET histograms of RT bound to PPT:d2 substrates in the presence of 0, 10, and 100 μM Nevirapine.